Electronic Supplementary Material (ESI) for Physical Chemistry Chemical Physics.

SUPPORTING INFORMATION

Double-Ring Tubular $(B_2O_2)_n$ Clusters (n=6-42) Rolled up from the Most Stable BO Double-Chain Ribbon in Boron Monoxides

Wen-Juan Tian,[a] Xin-Xin Tian,*[,a] Yue-Wen Mu,[a] Hai-Gang Lu,[a] and Si-Dian Li*[,a]

Nanocluster Laboratory, Institute of Molecular Science, Shanxi University, Taiyuan 030006, China

Electronic mail: lisidian@sxu.edu.cn.

Figure S1. Optimized planar and tubular structures of $(B_2O_2)_n$ (n=6-12, 21, 42) with their relative energy in eV at the PBE0/6-311+G* level. The B atom is in blue and O in red.

Figure S2. Optimized alternative low-lying structures of $B_{12}O_{12}$, with their relative energy in eV at PBE0/6-311+G*. Also shown are the relative energies at the single-point CCSD(T)//PBE0/6-311+G* (in *italic*), TPSSh/6-311+G* (in curly brackets), and B3LYP/6-311+G* levels (in square brackets), respectively. The B atom is in blue and O in red.

Figure S3. AdNDP bonding patterns of $B_{14}O_{14}$ (**3**, D_{7h}) (a) and $B_{16}O_{16}$ (**4**, D_{8h}) (b) with their occupation numbers (ONs) indicated.

Figure S4. Simulated (a) IR, (b) Raman, and (c) UV-Vis spectra of D_{6h} $B_{12}O_{12}$ (**2**) at the PBE0/6-311+G* level.

Figure S5. Simulated photoelectron spectra of $B_{12}O_{12}^-$ on the basis of TD-PBE0 calculations. The simulations were done by fitting the distribution of the calculated VDEs with unit-area Gaussian functions of 0.04 eV half-width.

Table S1. Optimized coordinates ((x, y, z) in Å) of tubular $(B_2O_2)_n$ (n=6-9) at the PBE0/6-311+G* level.

Figure S1. Optimized planar and tubular structures of $(B_2O_2)_n$ (n=6-12, 21, 42) with their relative energy in eV at the PBE0/6-311+G* level. The B atom is in blue and O in red.

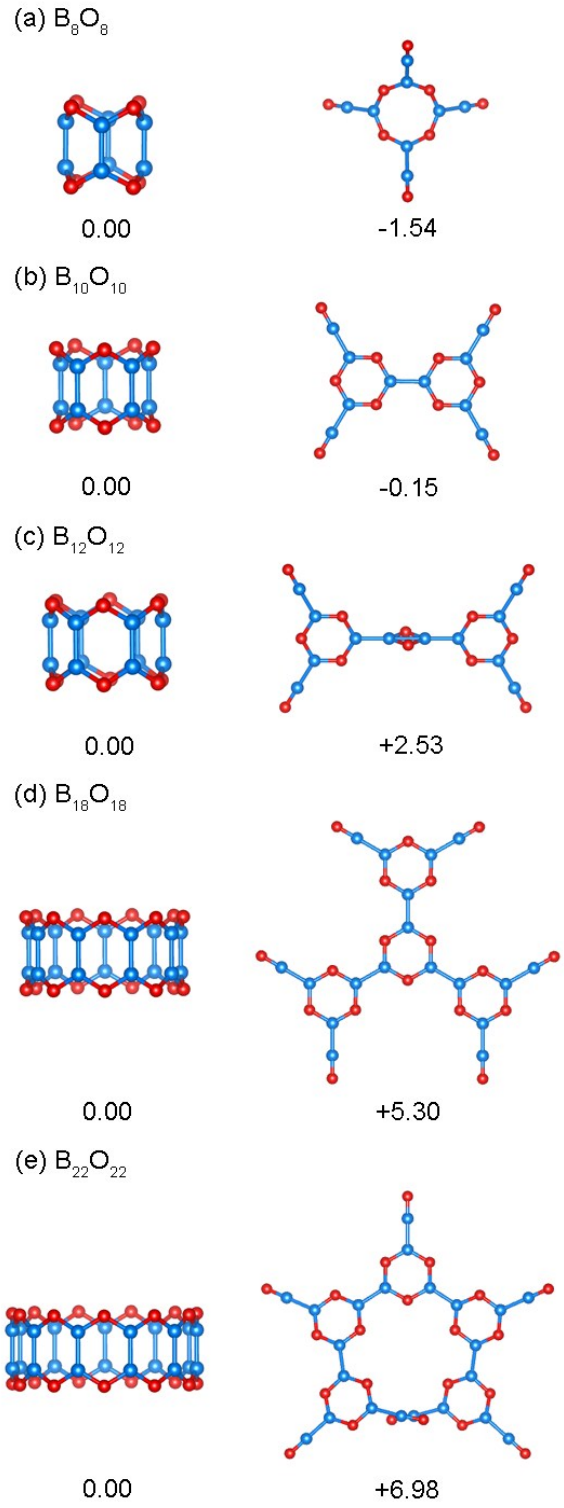

(f) $B_{24}O_{24}$

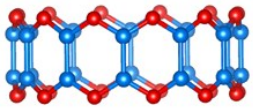

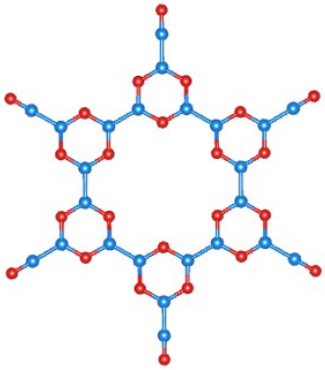

0.00 +6.06

(g) $B_{42}O_{42}$

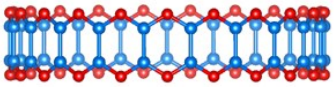

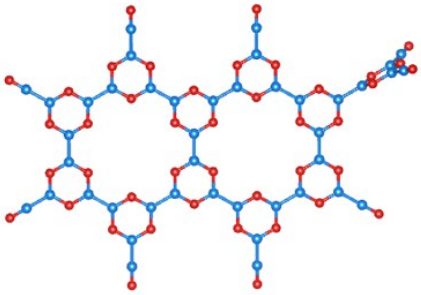

0.00 +11.35

(h) $B_{84}O_{84}$

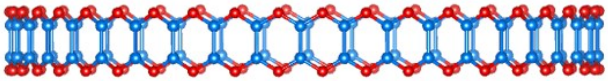

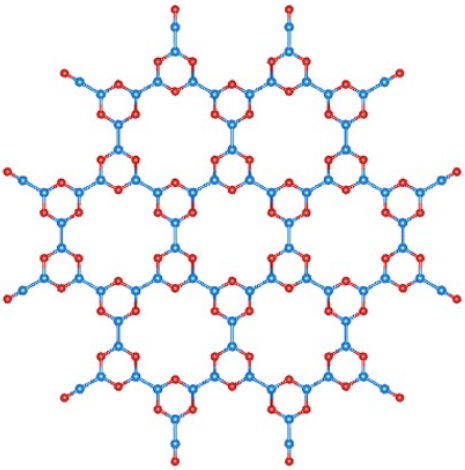

0.00 +17.22

Figure S2 Optimized alternative low-lying structures of $B_{12}O_{12}$, with their relative energy in eV at PBE0/6-311+G*. Also shown are the relative energies at the single-point CCSD(T)//PBE0/6-311+G* (in *italic*), TPSSh/6-311+G* (in curly brackets), and B3LYP/6-311+G* levels (in square brackets), respectively. The B atom is in blue and O in red.

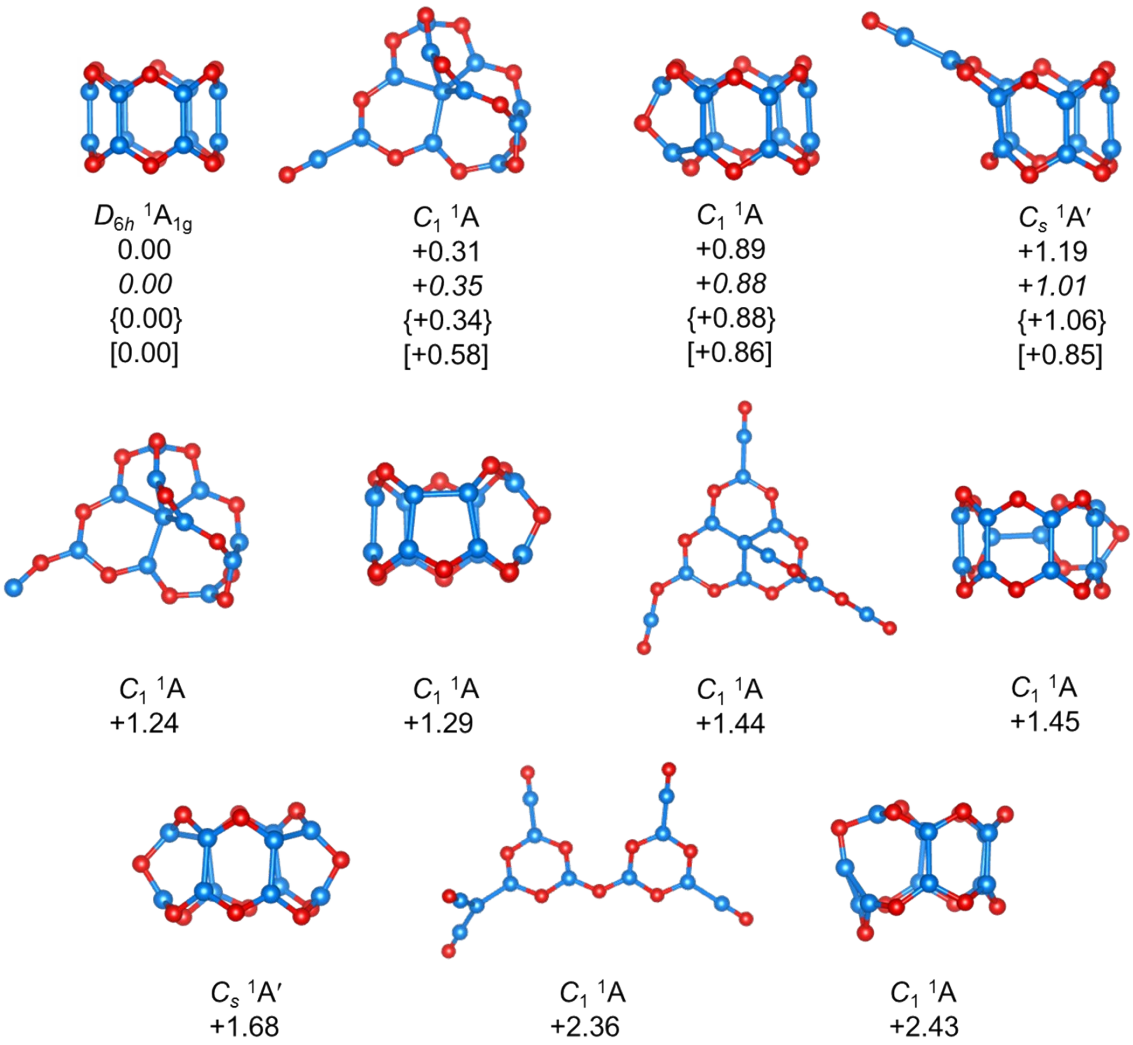

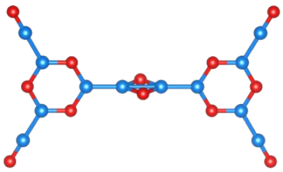

C_{2v} $^1A_1$
+2.53
+1.71
{+1.96}
[+1.16]

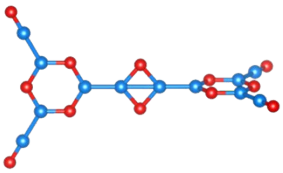

C_{2v} $^1A_1$
+2.54
+1.81
{+1.97}
[+1.18]

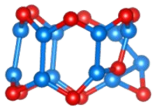

C_1 ^1A
+2.55

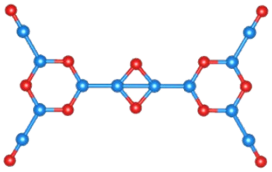

D_{2h} ^1A_g
+2.56
+1.84
{+2.00}
[+1.20]

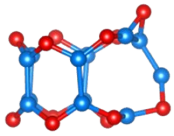

C_1 ^1A
+2.67

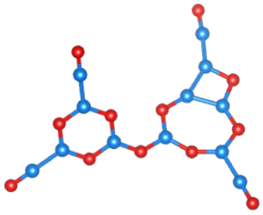

C_1 ^1A
+2.87

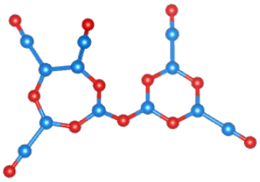

C_1 ^1A
+2.93

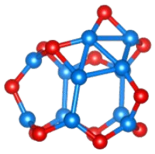

C_1 ^1A
+2.95

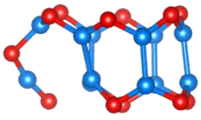

C_1 ^1A
+3.04

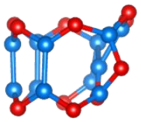

C_1 ^1A
+3.07

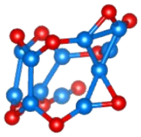

C_1 ^1A
+3.24

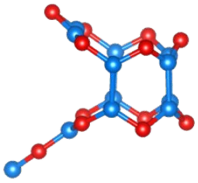

C_1 ^1A
+3.32

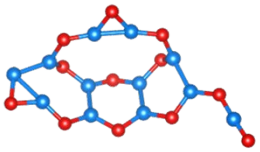

C_1 ^1A
+3.41

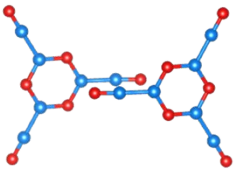

C_{2h} ^1A_g
+3.64

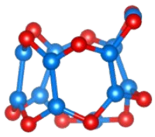

C_1 ^1A
+3.84

Figure S3. AdNDP bonding patterns of $B_{14}O_{14}$ (**3**, D_{7h}) (a) and $B_{16}O_{16}$ (**4**, D_{8h}) (b) with their occupation numbers (ONs) indicated.

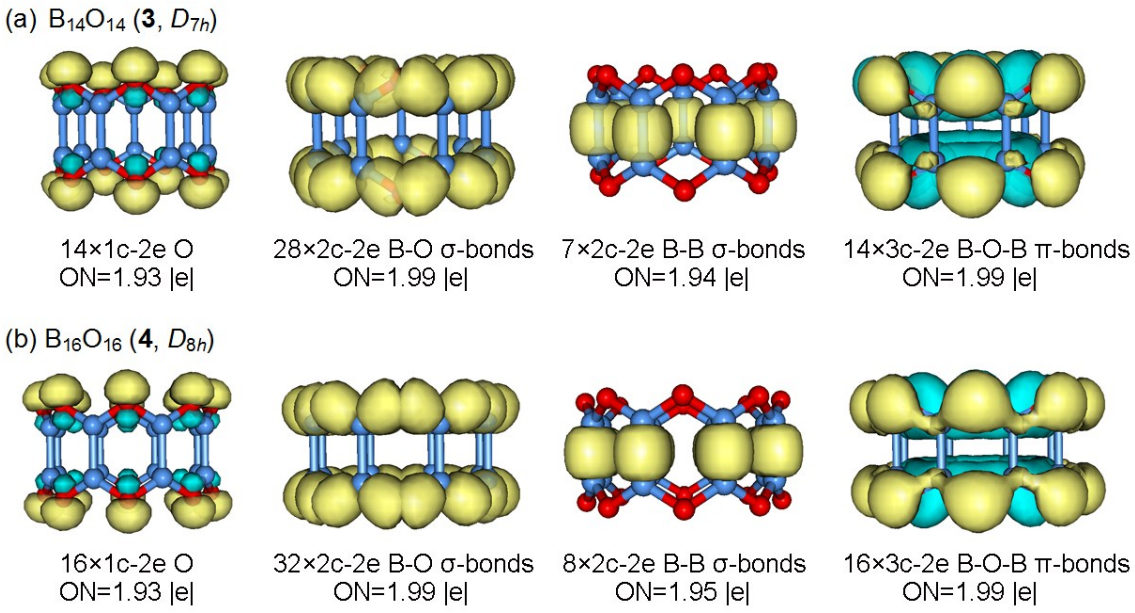

Figure S4. Simulated (a) IR, (b) Raman, and (c) UV-Vis spectra of D_{6h} $B_{12}O_{12}$ (**2**) at the PBE0/6-311+G* level.

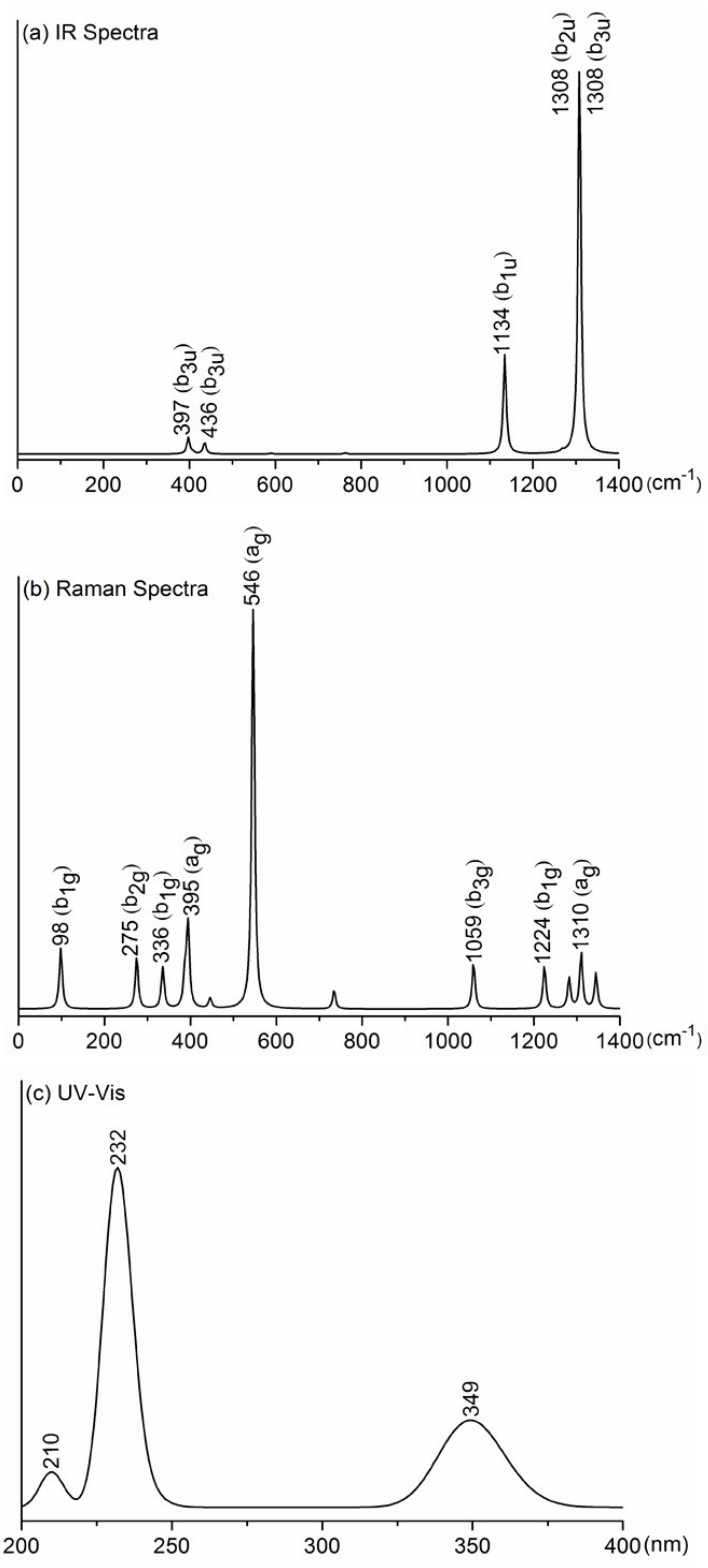

Figure S5. Simulated photoelectron spectra of $B_{12}O_{12}^-$ on the basis of TD-PBE0 calculations. The simulations were done by fitting the distribution of the calculated VDEs with unit-area Gaussian functions of 0.04 eV half-width.

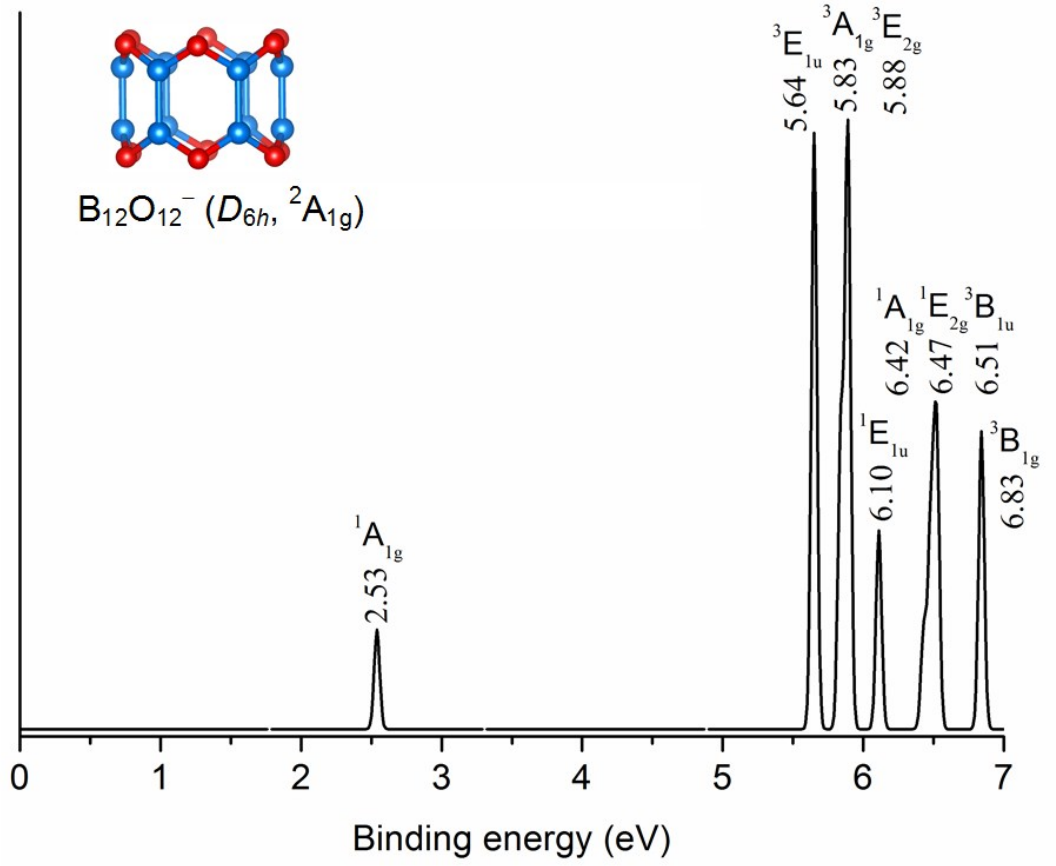

Table S1. Optimized coordinates ((x, y, z) in Å) of tubular $(B_2O_2)_n$ (n=6-9) at PBE0/6-311+G*.

D_{6h} $B_{12}O_{12}$ (**2**)

B	0.00000000	2.20361000	0.86953500
B	-1.90838224	1.10180500	0.86953500
B	-1.90838224	-1.10180500	0.86953500
B	0.00000000	-2.20361000	0.86953500
B	1.90838224	-1.10180500	0.86953500
B	1.90838224	1.10180500	0.86953500
B	1.90838224	-1.10180500	-0.86953500
B	-0.00000000	-2.20361000	-0.86953500
B	1.90838224	1.10180500	-0.86953500
B	-0.00000000	2.20361000	-0.86953500
B	-1.90838224	1.10180500	-0.86953500
B	-1.90838224	-1.10180500	-0.86953500
O	-1.18433138	2.05132212	1.55952800
O	1.18433138	2.05132212	1.55952800
O	-2.36866276	0.00000000	1.55952800
O	1.18433138	-2.05132212	1.55952800
O	-1.18433138	-2.05132212	1.55952800
O	2.36866276	0.00000000	1.55952800
O	1.18433138	-2.05132212	-1.55952800
O	1.18433138	2.05132212	-1.55952800
O	-2.36866276	0.00000000	-1.55952800
O	-1.18433138	2.05132212	-1.55952800
O	-1.18433138	-2.05132212	-1.55952800
O	2.36866276	0.00000000	-1.55952800

D_{7h} $B_{14}O_{14}$ (**3**)

O	1.18158653	2.45358971	-1.56446001
O	-1.18158653	2.45358971	-1.56446001
O	-2.65500084	0.60598662	-1.56446001
O	-2.12914536	-1.69793676	-1.56446001
O	-0.00000000	-2.72327913	-1.56446001
O	2.12914536	-1.69793676	-1.56446001
O	2.65500084	0.60598662	-1.56446001
O	-1.18158653	2.45358971	1.56446001

O	1.18158653	2.45358971	1.56446001
O	2.65500084	0.60598662	1.56446001
O	2.12914536	-1.69793676	1.56446001
O	0.00000000	-2.72327913	1.56446001
O	-2.65500084	0.60598662	1.56446001
O	-2.12914536	-1.69793676	1.56446001
B	0.00000000	2.57617591	-0.86848700
B	2.01413543	1.60621941	-0.86848700
B	2.01413543	1.60621941	0.86848700
B	0.00000000	2.57617591	0.86848700
B	-2.01413543	1.60621941	0.86848700
B	-2.01413543	1.60621941	-0.86848700
B	-2.51158580	-0.57325307	-0.86848700
B	-2.51158580	-0.57325307	0.86848700
B	-1.11776084	-2.32105430	-0.86848700
B	1.11776084	-2.32105430	-0.86848700
B	2.51158580	-0.57325307	-0.86848700
B	-1.11776084	-2.32105430	0.86848700
B	1.11776084	-2.32105430	0.86848700
B	2.51158580	-0.57325307	0.86848700

D_{8h} $B_{16}O_{16}$ (**4**)

B	0.00000000	2.95153900	0.86784500
B	-2.08705300	2.08705300	0.86784500
B	-2.95153900	0.00000000	0.86784500
B	-2.08705300	-2.08705300	0.86784500
B	0.00000000	-2.95153900	0.86784500
B	2.08705300	-2.08705300	0.86784500
B	2.95153900	0.00000000	0.86784500
B	2.08705300	2.08705300	0.86784500
B	2.08705300	2.08705300	-0.86784500
B	0.00000000	2.95153900	-0.86784500
B	-2.08705300	2.08705300	-0.86784500
B	-2.95153900	0.00000000	-0.86784500
B	-2.08705300	-2.08705300	-0.86784500
B	0.00000000	-2.95153900	-0.86784500
B	2.08705300	-2.08705300	-0.86784500
B	2.95153900	0.00000000	-0.86784500
O	2.84809500	1.17972000	-1.56753000

O	2.84809500	-1.17972000	-1.56753000
O	1.17972000	-2.84809500	-1.56753000
O	-1.17972000	-2.84809500	-1.56753000
O	-2.84809500	-1.17972000	-1.56753000
O	-2.84809500	1.17972000	-1.56753000
O	-1.17972000	2.84809500	-1.56753000
O	1.17972000	2.84809500	-1.56753000
O	2.84809500	-1.17972000	1.56753000
O	1.17972000	-2.84809500	1.56753000
O	-1.17972000	-2.84809500	1.56753000
O	-2.84809500	-1.17972000	1.56753000
O	-2.84809500	1.17972000	1.56753000
O	-1.17972000	2.84809500	1.56753000
O	1.17972000	2.84809500	1.56753000
O	2.84809500	1.17972000	1.56753000

D_{9h} $B_{18}O_{18}$ (**5**)

B	0.00000000	-3.32796990	-0.86740500
B	-2.13917782	-2.54937285	-0.86740500
B	-3.27741056	-0.57789591	-0.86740500
B	-2.13917782	-2.54937285	0.86740500
B	0.00000000	-3.32796990	0.86740500
B	2.13917782	-2.54937285	0.86740500
B	3.27741056	-0.57789591	0.86740500
B	-3.27741056	-0.57789591	0.86740500
B	-2.88210647	1.66398495	-0.86740500
B	-1.13823274	3.12726875	-0.86740500
B	-2.88210647	1.66398495	0.86740500
B	-1.13823274	3.12726875	0.86740500
B	1.13823274	3.12726875	-0.86740500
B	2.88210647	1.66398495	-0.86740500
B	1.13823274	3.12726875	0.86740500
B	2.88210647	1.66398495	0.86740500
B	3.27741056	-0.57789591	-0.86740500
B	2.13917782	-2.54937285	-0.86740500
O	3.39193894	0.59809035	-1.56960600
O	2.98282105	-1.72213253	-1.56960600
O	1.17800803	-3.23655047	-1.56960600
O	-1.17800803	-3.23655047	-1.56960600

O	-2.98282105	-1.72213253	-1.56960600
O	-3.39193894	0.59809035	-1.56960600
O	-2.21393091	2.63846012	-1.56960600
O	-0.00000000	3.44426507	-1.56960600
O	2.21393091	2.63846012	-1.56960600
O	3.39193894	0.59809035	1.56960600
O	2.98282105	-1.72213253	1.56960600
O	1.17800803	-3.23655047	1.56960600
O	-1.17800803	-3.23655047	1.56960600
O	-2.98282105	-1.72213253	1.56960600
O	-3.39193894	0.59809035	1.56960600
O	-2.21393091	2.63846012	1.56960600
O	0.00000000	3.44426507	1.56960600
O	2.21393091	2.63846012	1.56960600